JOURNAL OF MATERIALS SCIENCE 21 (1986) 2915–2925

Tertiary creep and ductile fracture in Al–Zn alloy: a consequence of structure development

MARIA A. MORRIS*, BRIAN SENIOR
Institut de Génie Atomique, Ecole Polytechnique Fédérale de Lausanne, CH-1015 Lausanne, Switzerland

The cause of failure in ductile materials has been, for many years, related to the presence of cavities. However, although large cracks or cavities have been associated with final fracture, direct observation of very small cavities throughout the neck development in pure metals or solid solution alloys has never been made. Cavity nucleation requires the existence of large local effective stresses for long enough periods of time. The different stages of necking in an Al–11 wt% Zn alloy were studied since it is known that large effective stresses are produced at sub-boundaries during the secondary stage of creep. No cavities were observed. Instead, the boundaries support large effective stresses which continue to be relaxed by dislocation emission throughout all the neck development. The subgrain size decreases from about 20 μm at the onset of tertiary creep to about 0.6 μm at the tip of the broken specimen at the same time as the stress continuously rises due to the large reduction in section throughout the neck. The presence of coarse slip bands from the beginning of the tertiary stage is related to strain localization as the high effective stresses lead to sub-boundary breakthrough and localized extensive dislocation activity. Fracture of the specimen occurs by shear and microcrack development following the localized softening associated with sub-boundary destruction.

1. Introduction

Brittle creep fracture is reasonably associated with the formation of cracks or cavities associated predominantly with stress or strain concentrations at grain boundaries. The fracture mode of ductile materials in cold deformation and creep has been studied over the past 30 years and while much emphasis has been put on the final stage of failure associated with cracks or cavities, very little work has been done on microstructure formation during the neck development. It is difficult to develop an accurate theory of fracture in the absence of precise information on deformation-induced substructure changes.

The literature on theories of cavity nucleation and growth is extensive. A major aspect of cavity nucleation is the need for large effective stresses: below a threshold value no nucleation is possible. Therefore, generally, grain boundaries are considered as the most favourable sites for cavity nucleation. However, during the deformation process a dislocation structure builds up, local effective stresses may exist. For example, for an applied stress of 11 $MN m^{-2}$ local effective shear stresses as high as 64 $MN m^{-2}$ were previously measured at sub-boundaries [1] during the secondary stage of creep. Their influence in the fracture process needs to be taken into account. For this reason, before a complete understanding of neck development and rupture of a ductile material can be obtained, it is necessary to study the evolution of the structure during deformation and its influence on the final rupture of the specimen.

As early as 1961, Beevers and Honeycombe [2] made observations on the surface of fractured copper and aluminium single and polycrystals in order to understand how pure metals with no inclusions would rupture. They reported the existence of coarse slip bands on the final stages of necking within which microcracks initiated. Since these cracks did not originate at inclusions, they assumed that a dislocation mechanism contributed to ductile fracture. The mechanism of rupture was attributed to the direct formation of microcracks by shear. Much more recently, Watanabe [3] has oberved cracks or cavities on grain boundaries of copper bicrystals crept to fracture. He related the mechanism of cavity formation to grain-boundary sliding in order to explain the large stress concentrations needed which in pure materials could not otherwise be attained. Since these cracks on the fractured surface were related to slip traces and sliding direction, he concluded that deformation ledges were potential sites for stress concentrations. Random grain boundaries slide more easily than coincidence boundaries and he emphasized the dependence of intergranular fracture on the types of boundaries present in the material.

Vergazov and Rybin [4] have made a complete study of microcracks produced by fracture in molybdenum under tensile deformation both by SEM and TEM. Their observations show that small elongated cracks, about 100 nm, in the direction of the tensile axis, appear on the fractured surface and that some of these cracks are also present at the sub-boundaries

* *Present address*: Institute of Structural Metallurgy, University of Neuchâtel, Av. de Bellevaux 51, Neuchâtel, Switzerland.

0022–2461/86 $03.00 + .12

produced by the deformation process at the final stages of necking. They did not observe any cavities in the neck region before failure.

Chang and Asaro [5] studied the fracture surface of Al–Cu alloys and observed coarse slip bands that preceded the appearance of macroscopic shear bands. Within these, they detected microcracks which joined to cause fracture. The presence of lattice rotations within the macroscopic bands was in agreement with the prediction of a previous theoretical model by Asaro [6]. They concluded that fracture occurred by geometrical softening within the bands due to the increase in the Schmidt factor as crystal rotation occurred inside the band. An interesting observation was that voids did not readily form in the interior of the shear bands, at least until complete specimen fracture was imminent.

Goods and Nix [7] observed the coalescence of cavities formed after diffusing water vapour into silver single crystals which were, then, crept to fracture. These cavities formed at grain boundaries and their coalescence led to final fracture of the specimen. However, this only confirms the growth of existing cavities during creep, since these cavities had been previously created by a method other than the deformation process, and therefore the strain-induced nucleation of cavities in ductile materials has yet to be confirmed.

The aim of the work was, then, to use an alloy in which the structure evolution throughout the primary and secondary stages of creep was already known and to produce further specimens for creep fracture studies. In this way the evolution of structure throughout the neck onset and development could be followed as a means to understand ductile fracture. The alloy was Al–11 wt % Zn from which recent microscopic observations have revealed interesting features about the deformation mechanisms occurring during secondary creep [1, 8, 9]. In particular, it was shown that the subgrain boundaries accumulate dislocations with increasing strain such that large local effective stresses are built up. A stochastic distribution of these positive and negative stresses exists which can be relaxed by dislocation emission from sub-boundaries. These local effective stresses increase for increasing strain and for higher applied stress. Even though the strain rate is constant during the secondary stage, the structure is not: the sub-boundary mesh size decreases and the misorientation between subgrains increases with strain as the effective stresses and the proportion of boundaries that can emit dislocations increase. This indicates the capability of the material structure to evolve as it deforms, as a means to release the energy stored during plastic strain. Under these circumstances how will neck development and final failure occur?

2. Experimental techniques

The alloy was the same Al–11 wt % Zn studied previously [1, 8, 9]. The major impurities were copper (27 p.p.m.), iron (8 p.p.m.); a small number of inclusions were observed on polished sections, but in no cases did these influence the final failure process. The polycrystals had about 1 mm grain size. Nine different specimens with a gauge length of 17 mm and gauge diameters ranging from 3 to 3.8 mm were creep tested. The reason for the diameter variation was that samples were in some cases electrolytically polished to different extents or in other cases not polished at all after machining in order to relate the influence of the surface roughness and variation of section to strain rate acceleration and final strain fracture.

The creep tests were performed in a constant stress machine provided with a cam such that its profile allowed the reduction of load as the specimen elongated and its section reduced. All the tests were performed at a stress of 10 MPa for which the strain rate in the secondary stage was $5 \times 10^{-6}\,\mathrm{sec}^{-1}$. The strain rate acceleration and necking started for all specimens at 35% true longitudinal strain and failure occurred at 54.5% nominal longitudinal strain. The reduction of area at fracture, was of course, much greater. To study the evolution of the structure during neck development, tests were stopped at different strains, namely 35%, 45%, 51% and 54.5% (fracture). For each strain two types of specimen were prepared: one for SEM observation and the second for TEM studies. The latter were rapidly cooled under load using the same technique as previously described [9]. Four different specimens were crept to failure to look for variations in the fracture process associated with structural differences; for example, grain size or orientation changes. In order to study the slip steps produced on the surface during the final stages of necking, one specimen was crept to 51% strain, cooled rapidly under load, polished before recreeping at the same stress. In this case the intermediate polish smoothed out the surface, removing the neck, and the specimen did not continue to creep with accelerating strain rate but instead crept under a constant strain rate of $4 \times 10^{-6}\,\mathrm{sec}^{-1}$.

Transmission electron microscopy (TEM) observations were made at 200 kV in foils prepared using a Struers Tenupol. In order to look for possible etching during foil preparation, two different electrolytes were used: 33% HNO_3–67% methanol and 10% perchloric acid–90% methanol. Foils were cut perpendicular to the tensile axis and also at 45° along the direction of the final rapid shear. At least ten foils from each type of specimen were observed in order to compare the structure in the neck region with that outside the neck and also to search for possible cavity formation. Sub-boundary misorientations and dislocation structures within the subgrains were examined using the procedures detailed previously [9], namely using several foil orientations and diffraction vectors. Scanning electron microscopy (SEM) observations of the specimens surfaces were made on both longitudinal and transverse sections.

Measurements of the minimum sections in the neck for each crept specimen were made both directly from the specimen by using a profile projector and indirectly from scanning electron micrographs. In the fractured specimens the sections were measured as a function of the distance from the broken tip. Since the loads were known in all cases, it was possible to calculate the true stress in the neck at the different stages of tertiary creep.

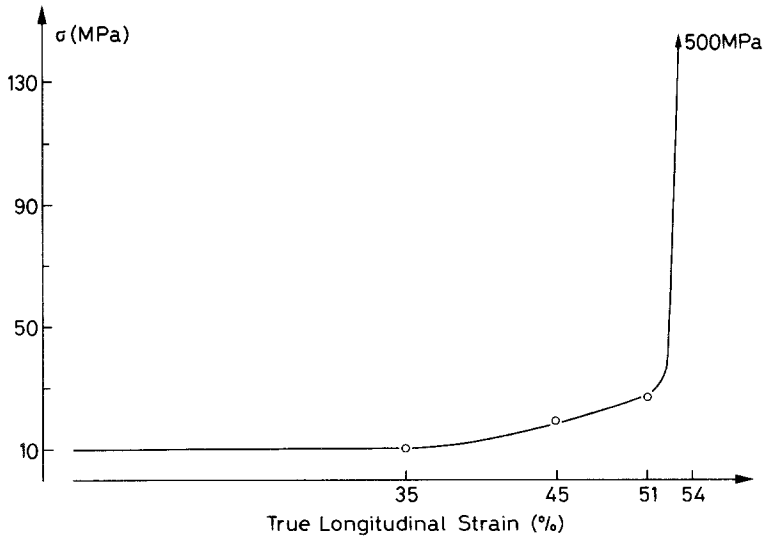

Figure 1 Calculated sectional stresses as a function of total longitudinal strain.

3. Results

The constant stress creep machine had a cam to reduce the load as the specimens elongated uniformly; the stress remained constant until the formation of a neck. From the values of the load at each instant and the measured minimum sections it was possible to calculate the maximum stresses in the neck. The results are shown in Table I and Fig. 1. The stress was uniformly 10 MPa along the specimen to 35% strain at which stage tertiary creep began. In the neck the local stress increased slowly from 10 to 26 MPa at 51% strain and the maximum local strain calculated from the reduction in area, $\ln(A_0/A_f)$, increased from 35% to 133%. However, during the very final stages of necking the stress rose very quickly such that after 54.5% longitudinal strain fracture occurred at a stress of 533 MPa and the maximum strain calculated from section reduction was 442%. In the case of the specimen given an intermediate polish and fractured at 74% true strain, the stress increased from 12 MPa at the beginning of the neck to 627 MPa at the fracture surface.

These local external stresses at different stages of necking must be kept in mind when the structure observations are related to the development of necking and fracture. Although tertiary creep began at 35% and fracture always occurred at 54.4% strain, the neck was not always produced in the same position: sometimes it occurred in the centre of the specimen, other times towards one of the ends. This suggests that the neck formation depends on the material microstructure.

Typical examples of a broken specimen and the fracture surface can be seen in Fig. 2. This figure shows the elongation of the grains in the direction of the tensile axis near and within the neck region, and the fracture surface produced perpendicular to the tensile axis. It is interesting to note the craters that form on both surfaces of the broken specimens. These craters suggest that local cavities or internal cracks may be responsible for the fracture process.

In order to determine the possible existence of cavities, the substructure was thoroughly examined in all the specimens tested and no evidence of cavities was found, either at grain boundaries or sub-boundaries. One of the foils cut perpendicular to the tensile axis from the specimen crept to 51% strain and after being polished with the perchloric–methanol mixture showed, however, preferential etch at one triple sub-boundary

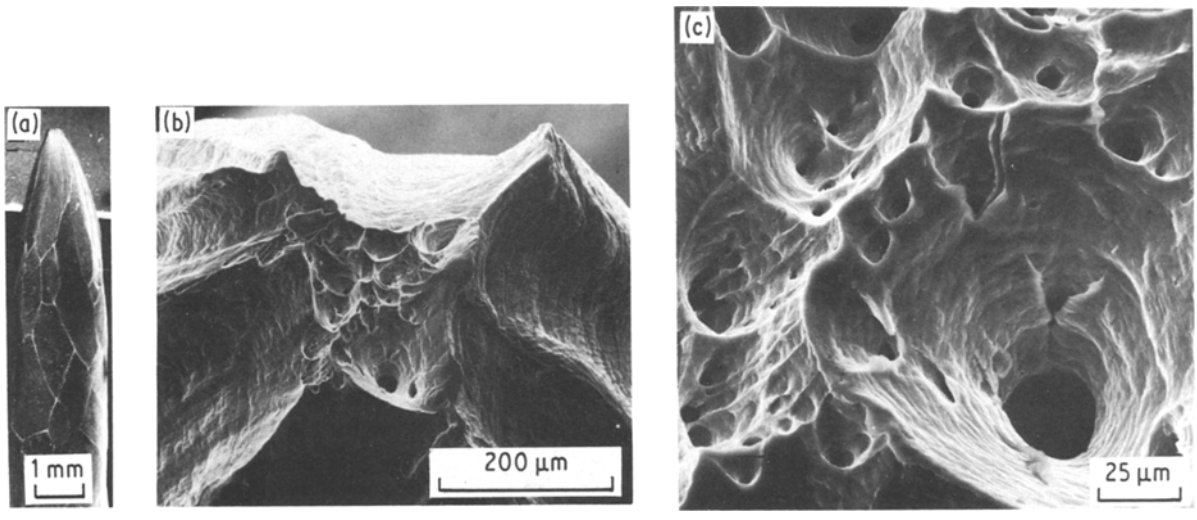

Figure 2 (a) Typical example of fractured specimen. (b) General view of fractured surface. (c) High magnification of holes or craters from (b).

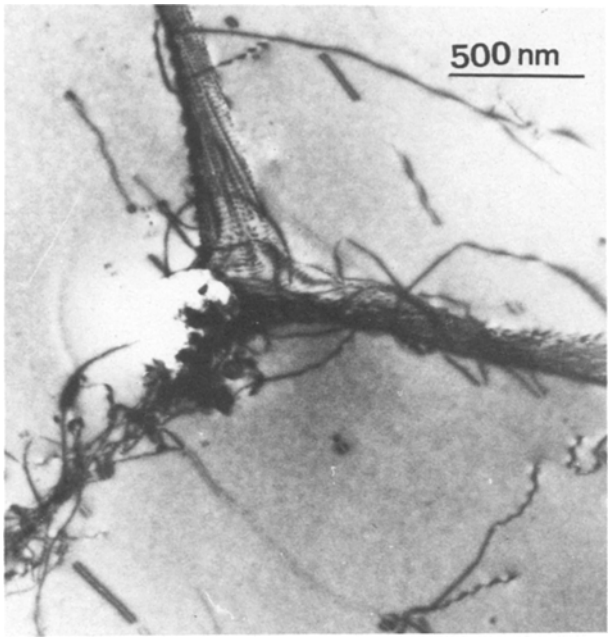

Figure 3 Triple junction under high effective stresses as a favourable site for etching (ε = 51%).

junction, as can be seen in Fig. 3. This figure shows that the local region of high stress, as indicated by the bowed dislocations, is a preferential site for etching which might be misinterpreted as being an original cavity. No other indication that cavities might be present in the material was found either by SEM or TEM examination.

3.1. TEM observations of substructure evolution

After 35% strain, when the tertiary stage begins, the sub-boundaries appear very dense producing large misorientations across them: this misorientation follows the same trend observed during the secondary stage (see [9]). The subgrain size has approximately the same value as that corresponding to the applied stress in previous studies of the secondary stage (i.e. $\simeq 20\,\mu$m). Bowed dislocation segments are still observed being emitted from very dense sub-boundaries all throughout the neck development up to 51% strain. Fig. 4 shows an example of this dislocation emission from the specimen crept to 45% deformation. The subgrain size appears to decrease slowly from 35% to 51% deformation. An example of some subgrains after 51% deformation can be seen in Fig. 5. The original subgrains about 19 μm in size appear subdivided into several smaller ones. This corresponds to the very large increase of stress in the neck region.

TABLE I

Longitudinal strain (%)	Section reduction strain (%)	Stress (MPa)
35	35	10
45	103	20
51	133	26
54.5	442	533

An important feature of the subgrain structure is that the misorientations produced across sub-boundaries oscillate between positive and negative values in a zig-zag manner such that the total misorientation around a 360° circuit is always equal to zero. These misorientations were determined by analysis of Kikuchi band displacements across each sub-boundary for several different foil orientations and therefore take account of the total misorientation. An example of such a group of subgrains is shown in Fig. 6. The misorientations across these boundaries varies from 0.12° to 1.05°. These low values of misorientations indicate that they are new sub-boundaries forming as the stress increases in the neck, since values of up to 2 to 3° had been previously measured after 15% deformation [9] and up to 6 to 7° after 35%. Rubtsov and Rybin [10, 11] have suggested that failure processes in ductile materials may be associated with disclination formation. In this case the rotation around such a circuit would not sum to zero. There is, therefore, no evidence to support the disclination theory of fracture. Since the total Burgers vector in the sub-boundary depends on the number and type of dislocations forming it, the accumulation or emission of dislocations from a boundary is not independent of other boundaries but is linked to them such that positive and negative rotations are associated to maintain a zero global rotation.

Another feature of the dislocation structure after large amounts of strain in the neck can be seen in Fig. 7. This shows two neighbouring subgrains observed in the neck region after 51% true strain. In one of the subgrains the dislocation density is extremely high whilst in the other, hardly any dislocations are present. This heterogeneity had already been observed within the secondary stage [9], and is an indication that the same mechanisms of deformation with soft and hard subgrains continues to exist throughout the neck development stage.

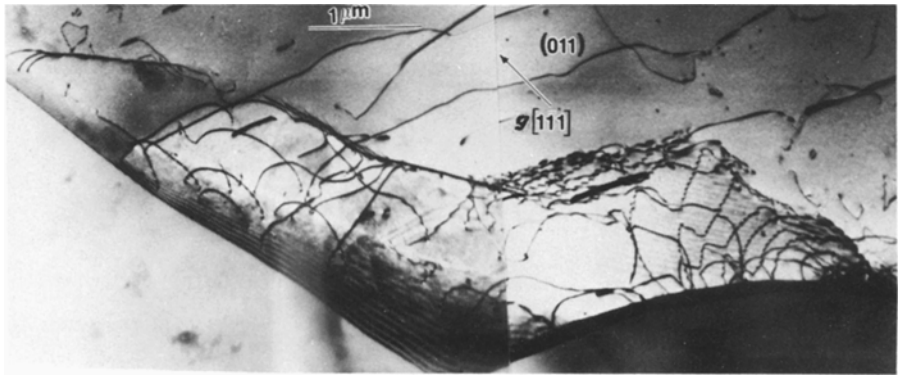

Figure 4 Dislocation emission from boundary in the neck (ε = 45%).

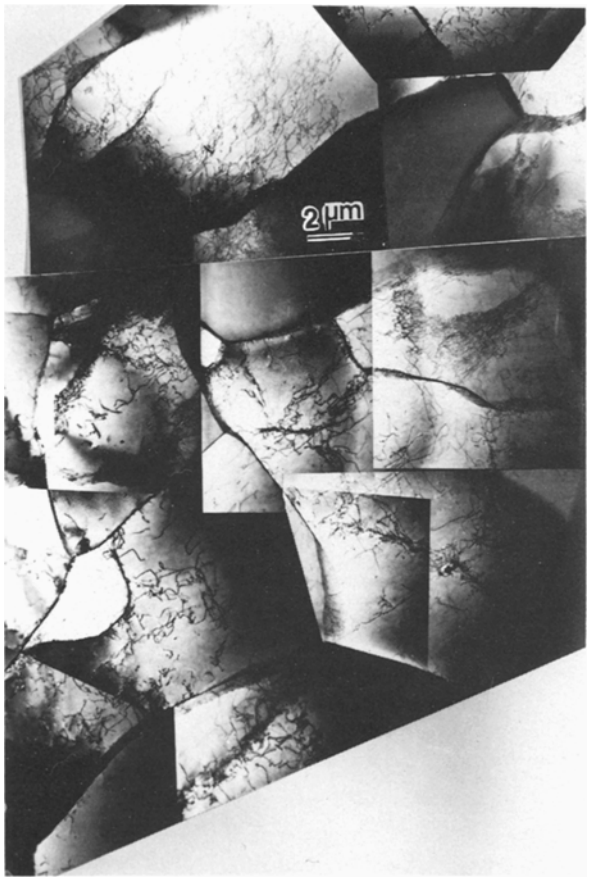

Figure 5 Typical subgrain structure in the neck (ε = 51%). One subgrain (bottom right) is subdivided into smaller subgrains.

Figs 8 and 9 show some examples of the structure observed in foils cut from the fractured specimens at about 600 μm from the broken tip. In Fig. 8, we see a characteristic subgrain size of about 0.6 to 2 μm typical of the corresponding cross-section and external stress for this advanced stage in the neck development. Stereo-pairs were taken from these types of subgrains and it was observed that sub-boundaries were always aligned along the tensile axis. Fig. 9 shows a pair of very dense sub-boundaries separated by less than 1 μm. Dislocation emission and propagation is very prominent indicating that the deformation process continues to be one of dislocation transfer between boundaries.

3.2. SEM observations

Subgrain size evolution was thoroughly studied on longitudinal and transverse sections. Fig. 10 shows some examples of subgrain size observed on the longitudinal cut surface of the fractured specimen as a function of the distance from the broken tip. In some cases larger subgrains containing smaller ones can be seen in agreement with TEM observations. Since the reduction in area and the corresponding stresses at those distances have been calculated, it has been possible to plot the subgrain size as a function of stress throughout the neck and just outside it. This plot is shown in Fig. 11. The subgrain size varies from about 14 μm at 3 mm from the tip where the stress was about 15 MPa to about 0.6 μm at 50 μm from the tip where the stress was 440 MPa. These values have been compared to those observed in transverse and longitudinal sections cut from specimens crept to 45% and 51% strain. The subgrain size measured after 45% deformation where the maximum stress in the minimum neck section was 20 MPa is about the same seen at 2.5 mm from the tip (i.e. $\simeq$ 12 μm) whilst the subgrain size measured in the minimum neck section of the specimen crept to 51% where the stress was 26 MPa corresponds to that observed at 1.5 mm from the broken tip (i.e. $\simeq$ 9 μm). This indicates that the subgrain structure evolves with stress as the neck region develops and that most of this evolution occurs in the final stages of necking as the stress rises fastest.

On the other hand, a different subgrain size dependence on stress is obtained compared to that seen during the secondary stage of creep in specimens crept at different stresses [1]. Whereas during secondary creep the subgrain size is inversely proportional to the square of the stress, $D \propto \sigma^{-2}$, in the neck region the subgrain size is inversely proportional to the stress, $D \propto \sigma^{-1}$. An important conclusion is that when the stress rises fast, the subgrain formation is not as rapid as that observed in specimens crept at different but constant stresses.

A rather interesting observation on the longitudinal section of the specimen crept up to 51% strain was the existence of a shear band at about 45° from the tensile axis across the specimen. The band was situated just outside the neck region and was connected to a notch on the surface of the specimen, as can be seen in Fig. 12a. This band was about 200 to 300 μm wide and consisted of elongated subgrains of a size about 8 μm along the direction of the band subdivided into smaller subgrains of a size approximately 1.5 μm in the transverse direction. Figs 12b and c show this band in detail where it can be seen that across each side of the band the subgrains are equiaxed and their size is about 16 μm. This shear band traverses all sub-boundaries and grain boundaries without distinction indicating the high intensity of the deformation front ahead of it. The shear band was, however, localized both in width and depth since repolishing to remove a layer of 200 μm removed practically all of the band and surface crack and only traces of the elongated subgrains were visible. The shear band was situated slightly outside the minimum neck section and seems to correspond to a longitudinal strain of 35%: this is the strain at which tertiary creep started. It seems likely that the reappearance of coarse slip steps (see next section) is the initial cause of this large shear band and this, in turn, leads to the surface notch formation.

3.3. Slips steps observations

Throughout the secondary stage of creep fine slip steps typical of homogeneous dislocation movement were present, in agreement with previous work [8]. The tertiary stage is characterized by the presence of coarse parallel slip lines characteristic of localized deformation. Fig. 13 shows some of these localized bands in one slip system that appeared traversing some of the subgrains from a distance of about 2.5 mm behind the broken tip corresponding to an external stress of 17 MPa. This means that localized, heterogeneous

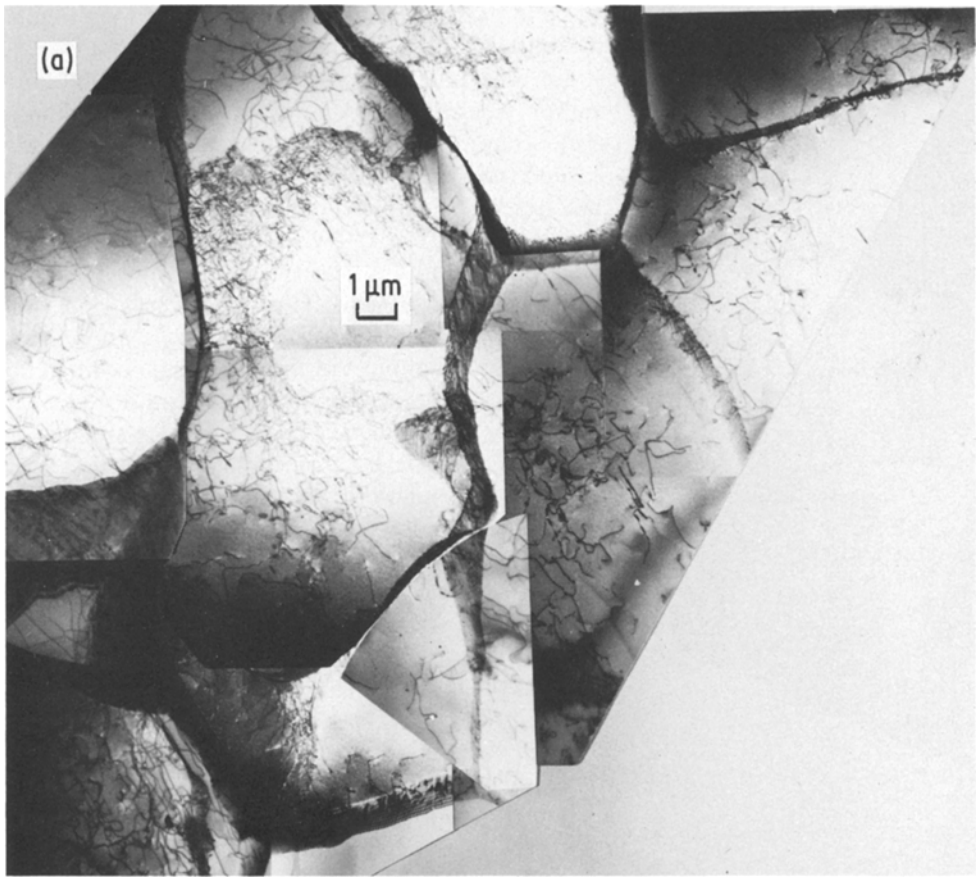

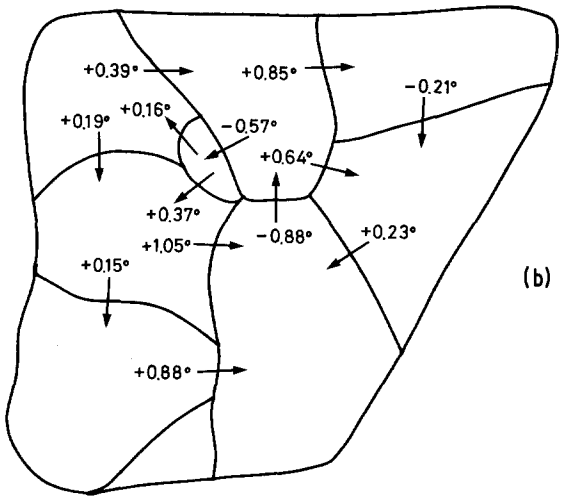

Figure 6 (a) New subgrains formed after 51% longitudinal strain producing low misorientations. (b) Reconstruction of (a) showing that any closed circuit produces zero total misorientation.

deformation appears again at the early stages of tertiary creep which is rather similar to that observed at the beginning of the primary stage. Some grain-boundary sliding is also visible. However, at this stage, the grain boundaries do not have a clear identity since, as shown in Fig. 14, they are diffused over a thickness of a few subgrains. The sliding does not then occur along a single boundary plane but rather in a zig-zag manner, where each sub-boundary migrates in turn. At about 1 mm from the broken tip, where the stress/strain is even greater, very pronounced bands in two slip systems appear as seen in Fig. 15, and thereafter the surface becomes so rough that subgrain contrast is no longer possible. Such localized intense deformation leads to the final fracture of the specimen.

4. Discussion

We try to understand the evolution of structure during neck development as a means to understand how ductile materials fail during creep. This discussion is of relevance to materials which are inherently ductile and where there are not the particles at boundaries which are frequently associated with failure nucleation. Most work done on fracture until now is related to the nucleation and growth cavities. However, cavities need large stress concentrations that must not relax if these are to grow. The structure observations presented here show that dislocation emission still occurs from boundaries where high effective stresses exist (see Figs 3, 4, 9) through most of the neck development. If the effective stresses can relax by dislocation emission, the stress concentration needed for cavity growth may never be possible. Thus no cavities were ever found because the stress concentrations never became sufficiently high. The cracks or holes found on the fracture surfaces of the broken tips have generally been related to a mechanism of cavity nucleation and growth. No proof of this has been found here. The microcracks observed are always elongated in the direction of the tensile axis in the same way as those observed by Vergazov and Rybin [4] and are only present on the final 200 μm of the neck. An example is given in Fig. 16 and suggests that the crack is associated with sub-boundaries since no grain boundary is present.

If we examine the evolution of the structure during

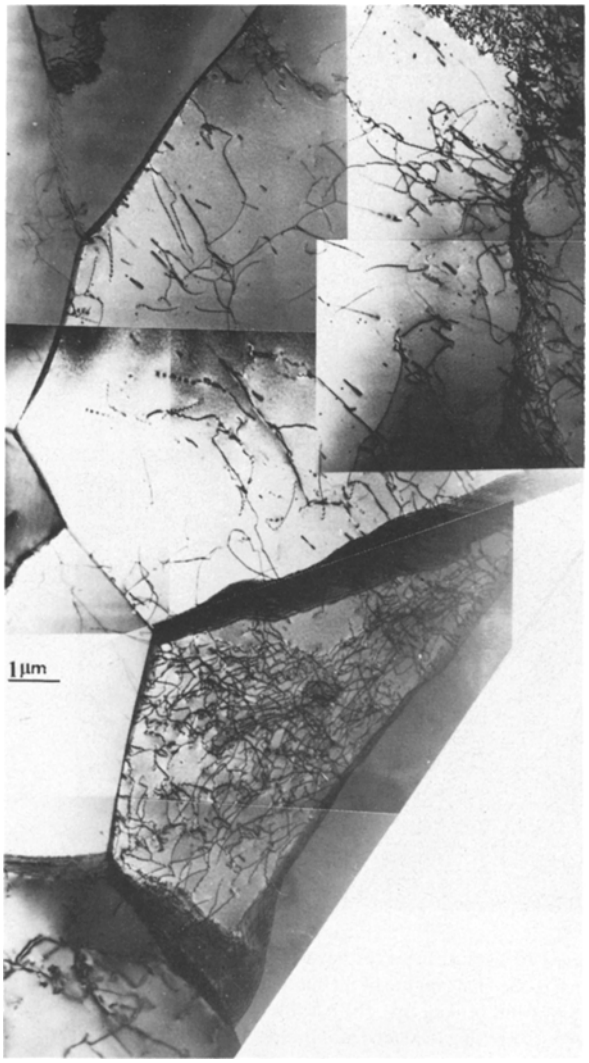

Figure 7 Two adjacent subgrains in the neck region (ε = 51%) showing high and low dislocation density.

tertiary creep, it is obvious that from the moment at which strain rate acceleration sets in, the material behaves in exactly the same way as when the stress is just applied; i.e. the increasing stress due to the reduction in section simply leads to an increase in strain rate and a structure that changes accordingly.

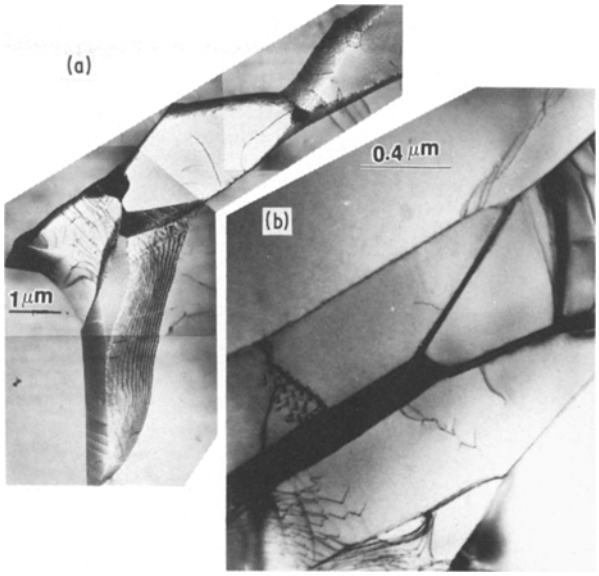

Figure 8 Subgrain structure observed at about 600 μm from the broken tip. (a) Foil plane perpendicular to tensile axis. (b) Foil plane at 45° from tensile axis.

The only difference between primary and tertiary creep is that in the former the stress rises suddenly, during application, but soon remains constant and the original very high strain rate soon decreases to a value characteristic of the structure corresponding to the maximum stress. In the tertiary stage, however, the rising stress does not stop rising and therefore the structure and strain rate continue to change.

Fracture in ductile materials finally occurs since the microstructure confers a resistance which is lower than the rising applied stress in the neck (i.e. the effective stresses at boundaries reach higher values than these boundaries can support, the number of mobile dislocations emitted will increase at a much higher frequency and a continuously accelerating creep rate is obtained). If the local effective stress rise too fast, complete deformation avalanches will occur, boundaries will locally disintegrate and the dislocations liberated move rapidly to the neighbouring sub-boundary. Since both original dense sub-boundaries

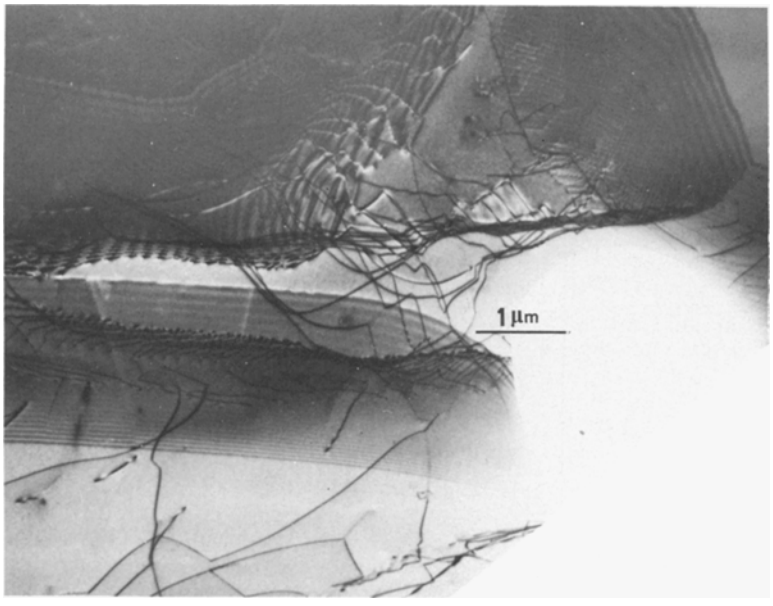

Figure 9 Dense sub-boundaries and dislocation emission observed in rupture specimen at about 500 μm from the broken tip.

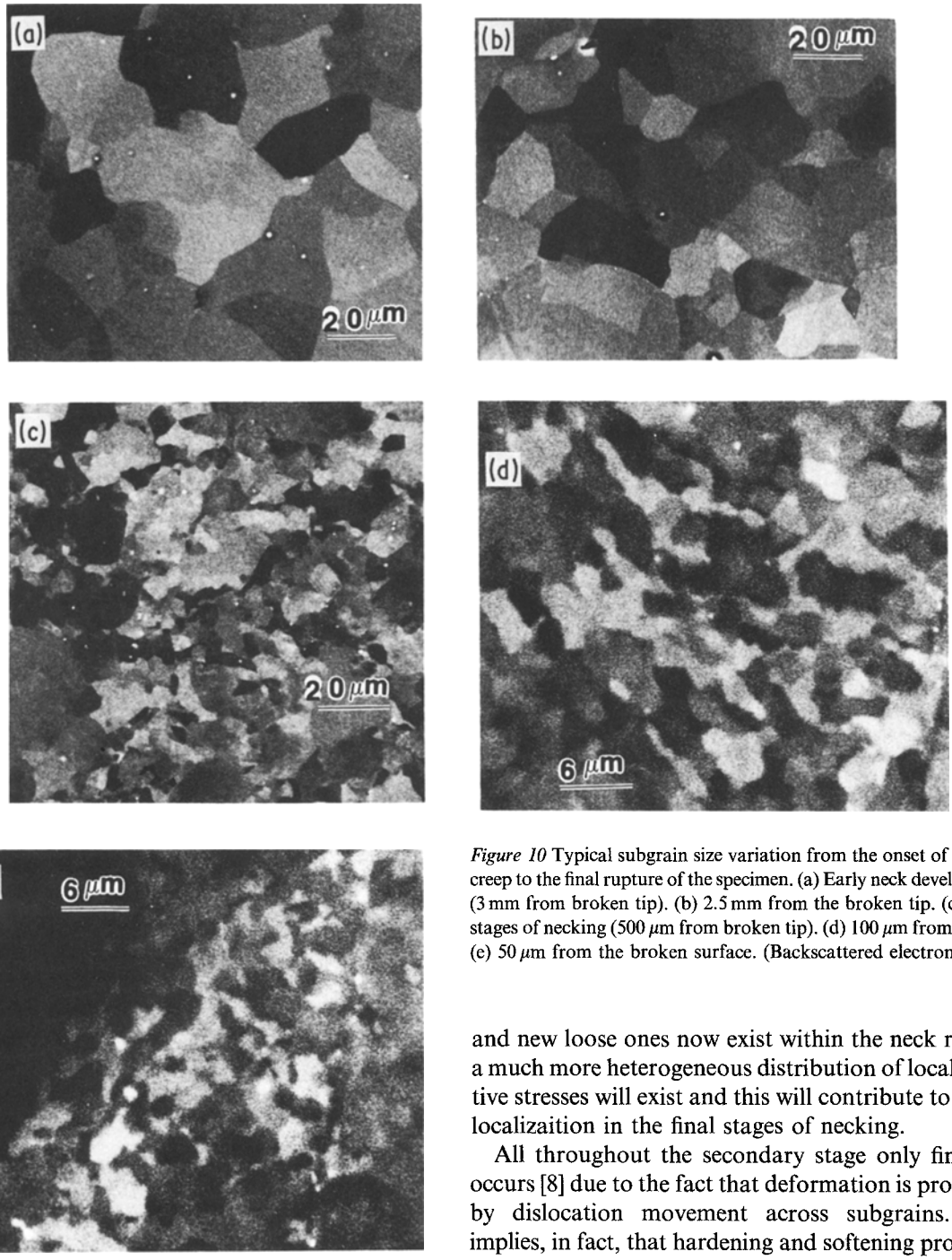

Figure 10 Typical subgrain size variation from the onset of tertiary creep to the final rupture of the specimen. (a) Early neck development (3 mm from broken tip). (b) 2.5 mm from the broken tip. (c) Later stages of necking (500 μm from broken tip). (d) 100 μm from the tip. (e) 50 μm from the broken surface. (Backscattered electrons.)

and new loose ones now exist within the neck region, a much more heterogeneous distribution of local effective stresses will exist and this will contribute to strain localizaition in the final stages of necking.

All throughout the secondary stage only fine slip occurs [8] due to the fact that deformation is produced by dislocation movement across subgrains. This implies, in fact, that hardening and softening processes

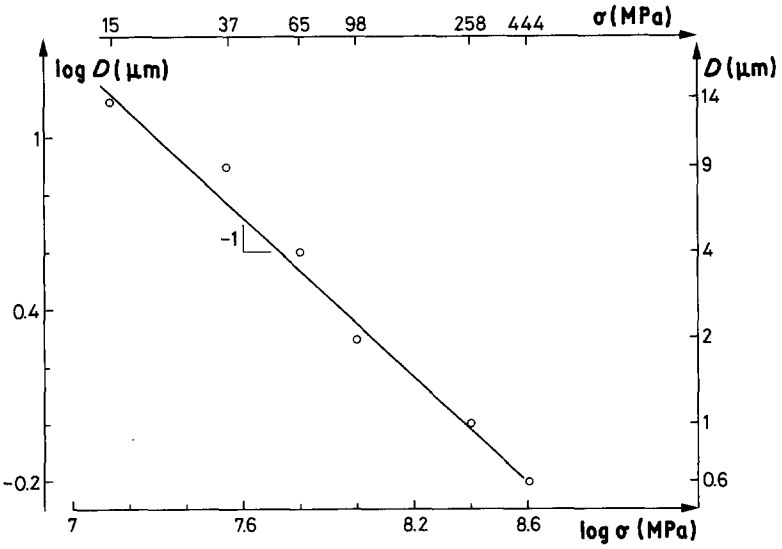

Figure 11 Double logarithmic plot of the subgrain size variation as a function of calculated stresses at different cross-sections in the neck.

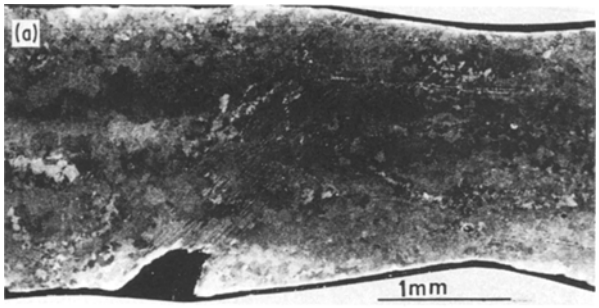

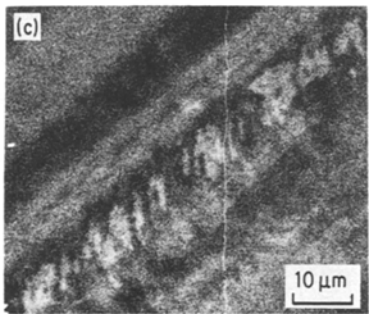

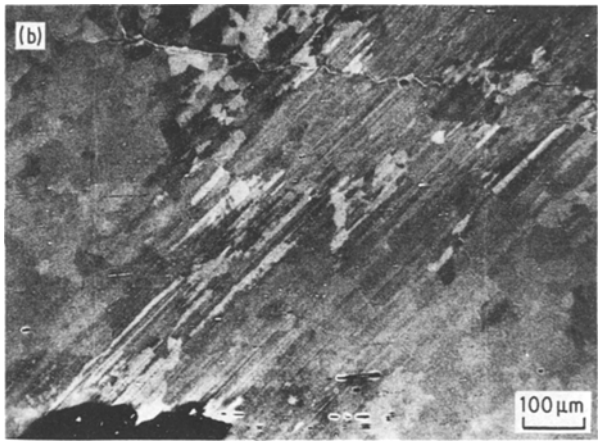

Figure 12 Shear band observed at 45° from tensile axis in longitudinal section of specimen crept to 51% true strain. (a) General view of neck region and band. (b) High magnification from bottom of (a) showing elongated subgrains in shear band. (c) Fine detail of small subgrains observed within elongated subgrains from (b). (Back-scattered electrons.)

can be identified as accumulation and emission of dislocations from sub-boundaries. As dislocation accumulation occurs at boundaries, the hardening increases and more softening becomes necessary (i.e. the boundaries contain more dislocations, become stronger obstacles and higher effective stresses are needed for dislocation emission to occur). Of course, there are also hardening and softening processes occurring at the subgrain interiors as observed by the subgrains containing large dislocation densities and those practically empty [9]. These hardening and softening processes occur intermittently across the specimen such that softening at a boundary (i.e. dislocation emission) cannot occur until the corresponding hard subgrain has softened by annihilation processes; however, at that time other sub-boundaries can be producing dislocation emission. In fact, what this simply means is that for a given strain rate only a certain number of mobile dislocations exist at a given time in the whole specimen due to the hardening and softening processes that fluctuate across it.

However, the appearance of new pronounced slip bands at the beginning of tertiary creep indicates the existence of preferential deformation in certain areas and, therefore, more softening processes. More dislocation emission occurs and their mean free path is longer: several subgrains can be traversed since not all sub-boundaries are sufficiently strong obstacles. These processes appear obvious under the action of the rising applied stresses which exist within a pre-existing neck. However, prior to tertiary creep the stress is constant and the existence of a sufficiently soft shear band can only be due to the structure formed during the secondary stage. Then intense slip bands are observed only in the region which eventually becomes the reduced-section neck region. Which arises first — intense slip bands or incipient necking? Clearly once the incipient neck occurs the localized reduction in area is not compensated by the cam

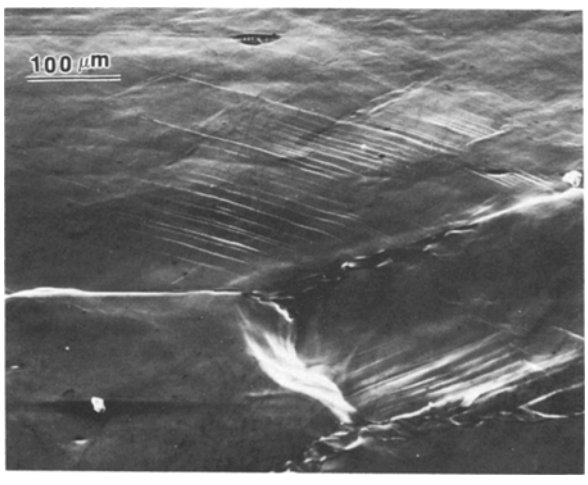

Figure 13 Localized slip steps observed from the onset of tertiary creep (ε = 45%).

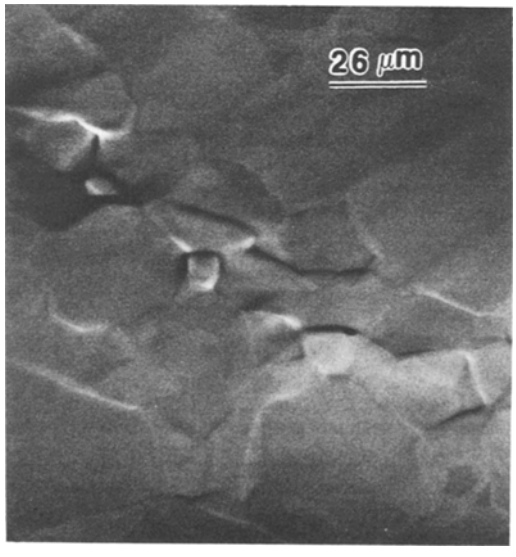

Figure 14 After large strains, grain boundaries lose their identity and appear made up of small subgrains (ε = 51%).

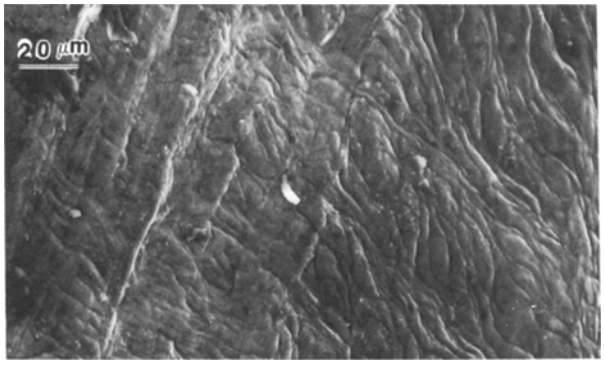

Figure 15 Very pronounced slip bands in two systems observed at about 1 mm from the broken tip.

system and the increase in local applied stress will maintain neck development.

Building up of the structure of a sub-boundary means accumulation of dislocations at boundaries which increases the misorientation and therefore the energy of the boundary. This increase in energy leads to high internal stresses which are responsible for dislocation emission and, thus, the deformation process. However, the energy of a boundary increases only up to a certain value of misorientation [12, 13]. Once the maximum value is reached, the energy decreases for any further increase in misorientation. Therefore, any dislocation accumulation that occurs after such a value of maximum energy will lead to an increase in misorientation but a decrease in the boundary energy. At this point there will be no more dislocation emission from the boundary. The moment will be reached at which many of these boundaries will not be able to emit dislocations and the few boundaries that can continue to do so will produce all the strain, thus strain localization will occur at those sites. This will give rise to local softening where an avalanche of dislocations will be produced leading to the appearance of localized slip bands. The creation of such a very intense band may eventually give rise to the observed concentrated shear band. Within this band, the very small subgrain size corresponds to a stress value of about 100 MPa indicating that the localized stress in this region is much higher than the corresponding stress of about 10 MPa calculated from the section of the specimen. This very high stress along the macroscopic shear band indicates that deformation occurs virtually instantaneously since the effective stresses needed for dislocations to traverse boundaries are already provided. This discussion is analogous to the theoretical predictions made by Asaro [6] and later confirmed experimentally [5] in which the lattice rotation produced within a shear band led to softening and strain localization. The contrast observed from small subgrains in the shear band formed prior to necking in our specimen indicates the large rotations produced with respect to the lattice.

Once the shear band propagates, it will reach the specimen surface and there the strain localization will create a microcrack. Throughout all this time the local applied stress increases. This will continue until eventually, microcracks form and large cracks lead to fracture.

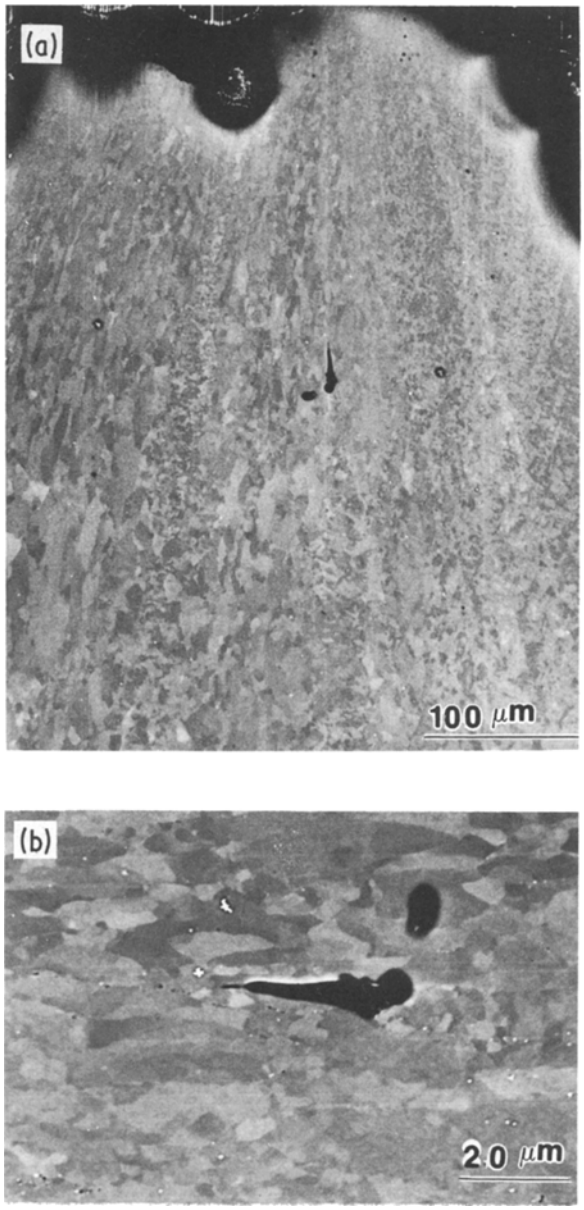

Figure 16 (a) Typical general subgrain structure and microcrack observed on longitudinal section of fractured specimen. (b) High magnification from microcrack region in (a). (Backscattered electrons.)

Therefore, the evolution of the creep process for such a ductile material is such that the controlling microstructural parameters such as subgrain size, sub-boundary mesh size and misorientations across subgrains will determine the material behaviour through the action of high local effective stresses from the moment the load is applied until the moment of rupture.

5. Conclusions

The evolution of structure throughout the neck development during creep has been studied. The subgrain size decreases with the decrease in section of the specimen due to the rising stresses. However the subgrain size dependence on stress is lower than that observed during the secondary stage for different specimens crept at different, constant stresses. Care should be taken when tests are performed at constant load since the effect of the rising stress during the secondary stage will modify the structure.

Dislocation accumulation at boundaries eventually produces very high misorientations, strain localization begins leading to coarse slip lines, eventually to a massive shear band and to necking. The strain localization may be associated with the achievement of a critical sub-boundary misorientation and energy.

No evidence for cavity nucleation and growth has been found on testing this ductile alloy in agreement with the idea that the high effective stresses can be relaxed by dislocation emission; therefore, nucleation of such cavities is not possible. The fracture occurs by shear and microcrack development after coalescence of sub-boundaries and not by cavity formation.

References

1. M. A. MORRIS and J. L. MARTIN, *Acta Metall.* **32** (1984) 1609.
2. C. J. BEEVERS and R. W. K. HONEYCOMBE, *Phil. Mag.* **7** (1962) 763.
3. T. WATANABE, *Met. Trans. A* **14A** (1983) 531.
4. A. N. VERGAZOV and V. V. RYBIN, *Fiz. Met. Metall.* **46** (1978) 371.
5. J. W. CHANG and R. J. ASARO, *Acta Metall.* **29** (1981) 241.
6. R. J. ASARO, *ibid.* **27** (1979) 445.
7. S. H. GOODS and W. D. NIX, *ibid.* **26** (1977) 751.
8. M. A. MORRIS, D. MASSON, B. SENIOR and J. L. MARTIN, *Scripta Metall.* **17** (1983) 687.
9. M. A. MORRIS and J. L. MARTIN, *Acta Metall.* **32** (1984) 549.
10. A. S. RUBTSOV and V. V. RYBIN, *Fiz. Met. Metall.* **44** (1977) 139.
11. V. V. RYBIN, *ibid.* **44** (1977) 623.
12. J. FRIEDEL, "Dislocations" (Pergamon Press, Oxford, 1964) p. 287.
13. J. VITEK and G. J. WANG, Proceedings of the Yamada Conference (1984) p. 637.

Received 26 September
and accepted 14 October 1985